Adaptive Target Detection across a Clutter Boundary: GLRT and Maximally Invariant Detectors

Hyung Soo Kim and Alfred O. Hero

Abstract— **We present and compare adaptive detection algorithms developed for synthetic aperture radar and imaging radar targets in structured clutter, utilizing both generalized likelihood ratio (GLR) tests and maximal invariant (MI) tests. We consider the problem of detecting a target straddling a known boundary of two independent regions inducing a clutter covariance matrix with block diagonal structure. GLR and MI tests are presented for various clutter scenarios: totally unknown clutter types, one of clutter types known except for its variance, and one of clutter types completely known. Numerical comparisons will illustrate that GLR tests and MI tests are complementary–neither test strategy uniformly outperforms the other–suggesting that it may be worthwhile to combine these tests for overall optimal performance.**

I. Introduction

In automatic target recognition, the most important issue is reliable detection which is robust to target and clutter variability, yet maintains the highest possible discrimination capability. In the past, most adaptive radar and array detection problems have been formulated under the general assumption that the target has known form but unknown amplitude in Gaussian noise whose covariance matrix is totally unknown or unstructured. The nature of this assumption led to the application of the generalized multivariate analysis of variance (GMANOVA) model to the parametric signal model, and the subsequent development of many detection algorithms. With this assumption and the GMANOVA model, Kelly [1] derived the constant false alarm rate (CFAR) test using the generalized likelihood ratio (GLR) principle and in so doing proved that the test is an invariant test as well.

However, one can expect an improvement in performance by exploiting a priori structure of the clutter covariance matrix, which must be estimated in the GLR test (GLRT). For adaptive arrays, Bose and Steinhardt [2] proposed an invariant detector which outperforms the Kelly's test when the clutter covariance matrix is assumed to have a certain known block diagonal structure. This work was the springboard in [3] for synthetic aperture radar (SAR) imaging target detection in the difficult deep hide scenario where the target parks along a known boundary separating two adjacent clutter regions. Indeed, under the assumption that the two clutter types are statistically independent, the spatial covariance has a block diagonal structure and this structure was used in [3] to derive another invariant test.

The authors are with the Dept. of Electrical Engineering and Computer Science, the University of Michigan, Ann Arbor, MI 48109-2122.

This work was supported in part by AFOSR under MURI grant: F49620-97-0028.

In this paper we extend the work reported in [3] by comparing the invariant method of [3] to the GLRT. Derivation of the GLRT for the case of structured covariance is not trivial, and the details are omitted due to space limitations. Here we compare the GLR tests to the invariant tests on the basis of simulation for the deep hide scenario.

II. GLR vs. Invariance Principles

Fig. 4 shows the magnitude part of a complex valued SAR clutter image of a rural scene consisting of two clutter types (forest canopy and grass field) separated by a boundary. The deep hide target detection problem treated in this paper is to detect a target that straddles the boundary. We make the assumptions that the complex clutter image is circular Gaussian with zero mean and that two spatial samples taken respectively from Region A and Region B are uncorrelated. By centering a 1-pixel wide vertical window with fixed vertical extent at the boundary (or its estimate) in Fig. 4 and sliding it over the image from left to right we obtain a reduced image (Fig. 6) with a horizontal boundary. Any of the clutter-alone image chips shown in Fig. 6 will be multivariate Gaussian with zero mean and covariance matrix $\mathbf{R}$ having block diagonal structure. The goal is to construct a test that a given chip contains clutter alone (H_0) vs. clutter plus target (H_1) where target spatial structure is known but its position and orientation along the boundary are unknown. We separate the clutter scenarios into three different cases:

- Case I: $\mathbf{R} = \begin{bmatrix} \mathbf{R}_A & \mathbf{O} \\ \mathbf{O} & \mathbf{R}_B \end{bmatrix}$
(unknown clutter in regions A and B)
- Case II: $\mathbf{R} = \begin{bmatrix} \mathbf{R}_A & \mathbf{O} \\ \mathbf{O} & \sigma^2\mathbf{I} \end{bmatrix}$
(clutter known in region B up to variance σ^2)
- Case III: $\mathbf{R} = \begin{bmatrix} \mathbf{R}_A & \mathbf{O} \\ \mathbf{O} & \mathbf{I} \end{bmatrix}$
(clutter known exactly in region B)

where $\mathbf{R}_A > 0$, $\mathbf{R}_B > 0$, and $\sigma^2 > 0$. Since there exists no uniformly most powerful test for these structured covariance matrices, the invariance principle is applied as well as the mainstay method of the GLR principle in an attempt to find the sub-optimal tests or CFAR tests. It can be shown that the GLR tests have explicit forms requiring rooting a complex quartic equation in the complex target amplitude parameter a. As described in [4], the maximal invariant (MI) test is constructed by applying the likelihood ratio test to a statistic called the *maximal invariant*. The maximal invariant is the lowest dimension statistic summarizing

the data yet preserving the target vs. clutter discrimination capability for the specific uncertainty structures of cases I, II, or III. Using the set of maximal invariant, Bose and Steinhardt [2] derived a MI test for Case II without target position uncertainty. MI tests for Case I and Case III can also be derived [2], [3].

For the GLR tests, numerical polynomial rooting was used to determine the unknown amplitude a and the resulting tests were compared to the invariant tests for each of the cases I, II, and III. GLR tests are listed in Table 1 where the measurement matrix is partitioned as

$$\mathbf{X} = \begin{bmatrix} \mathbf{X}_A \\ \mathbf{X}_B \end{bmatrix} = \begin{bmatrix} \underline{x}_{A1} & \mathbf{X}_{A2} \\ \underline{x}_{B1} & \mathbf{X}_{B2} \end{bmatrix},$$

where each column corresponds to pixel values in a different chip. The known target signature is $\underline{s} = \begin{bmatrix} \underline{s}_A^H & \underline{s}_B^H \end{bmatrix}^H$, and

$$\begin{aligned} p(a, \mathbf{X}_A) &= (\underline{x}_{A1} - a\underline{s}_A)^H (\mathbf{X}_{A2}\mathbf{X}_{A2}^H)^{-1} (\underline{x}_{A1} - a\underline{s}_A), \\ q(a, \mathbf{X}_B) &= tr\{(\mathbf{X}_B - a\underline{s}_B\underline{e}_1^H)^H (\mathbf{X}_B - a\underline{s}_B\underline{e}_1^H)\}. \end{aligned}$$

Here the subscripts denote the two different regions A and B, $\underline{x}_{A1}$ and $\underline{x}_{B1}$ denote pixels in the chip which is being tested for containing the target, and $\underline{e}_1$ is the unit vector.

TABLE I

GLR TESTS FOR VARIOUS BLOCK STRUCTURED CLUTTER COVARIANCE. (The notation '?' denotes 'unknown' quantity in the model)

$\mathbf{R}_A$	$\mathbf{R}_B$	Log GLR $(\frac{1}{n}\ln\Lambda = \max_a\{\cdot\})$
?	?	$\ln\left[\frac{1+p(0,\mathbf{X}_A)}{1+p(a,\mathbf{X}_A)}\right] + \ln\left[\frac{1+p(0,\mathbf{X}_B)}{1+p(a,\mathbf{X}_B)}\right]$
?	$\sigma^2\mathbf{I}$	$\ln\left[\frac{1+p(0,\mathbf{X}_A)}{1+p(a,\mathbf{X}_A)}\right] + \ln\left[\frac{q(0,\mathbf{X}_B)}{q(a,\mathbf{X}_B)}\right]$
?	$\mathbf{I}$	$\ln\left[\frac{1+p(0,\mathbf{X}_A)}{1+p(a,\mathbf{X}_A)}\right] + \frac{1}{n}\left[q(0,\mathbf{X}_B) - q(a,\mathbf{X}_B)\right]$

III. Numerical Comparisons

To analyze the performance of the GLR and MI tests derived under the three structured covariance assumptions, ROC curves are generated for all three cases. In Figs. 1-3, the probability of detection (P_D) is calculated empirically as a function of the probability of false alarm (P_{FA}) by varying thresholds on the GLR and MI tests. Note that the three GLR tests matched to one of the three cases are compared to each other and to the invariant tests: Kelly's GLR test matched to Case I, Bose and Steinhardt's MI test matched to Case II, and the MI test matched to Case I. In all cases, these figures confirm that the tests derived under the matched assumption outperform those which are mismatched.

Of particular interest, however, are the crossings in the low P_{FA} regions between the GLR tests and the MI tests. In Fig. 1, we can observe the gains in P_D of the MI test over GLRT 1 for $P_{FA} < 0.1$. Moreover, it should be noted that the structured Kelly's test is outperformed by the MI test in the low P_{FA} region and by GLRT 1 in the high P_{FA} region. For Case II, although Bose and Steinhardt's MI test outperforms all the other tests, it appears that GLRT 2 slightly outperforms this test for very low P_{FA} (Fig. 2 (a)). These observations also hold for mismatched cases: between the MI test and GLRT 1 in Case II/III (Figs. 2/3), and between GLRT 2 and Bose and Steinhardt's test in Case I/III (Figs. 1/3).

Next, we considered an application to the real image in Fig. 4. The boundary was hand extracted and a 9×7 SLICY target from Fig. 5 was inserted so that it straddles the boundary. With the realigned image in Fig. 6, the MI test and GLRT 1 statistics are calculated and maximized pixel by pixel (Fig. 7). Both tests detected the target in column 300, yet in this experiment GLRT 1 statistic exhibits a higher deflection at the target location.

IV. Conclusion

The deep hide scenario considered in this paper complicates the design of optimal target detectors. This scenario gives rise to block diagonal constraints imposed by the clutter covariance structure. Both GLR and MI tests can be derived under these constraints. Numerical results indicate that neither GLR nor MI tests dominate the other in terms of ROC performance. The relative advantages of GLR vs. MI tests depend on factors such as: the prescribed FA rate, the clutter-to-target power ratio, the window size, and the prior uncertainty in the spatial covariance. These issues will be more fully addressed.

References

[1] E. J. Kelly, "An adaptive detection algorithm," *IEEE Trans. Aerosp. Electron. Syst.*, vol. AES-22, pp. 115-127, Mar. 1986.

[2] S. Bose and A. O. Steinhardt, "A maximal invariant framework for adaptive detection with structured and unstructured covariance matrices," *IEEE Trans. Sig. Proc.*, vol. 43, no. 9, pp. 2164-2175, Sep. 1995.

[3] A. O. Hero and C. Guillouet, "Robust detection of SAR/IR targets via invariance," *1997 ICIP*, Santa Barbara, CA, vol. 3, pp. 472-475, Oct. 1997.

[4] T. Kariya and B. K. Sinha, *Robustness of Statistical Tests*, Academic Press, San Diego, 1989.

[5] P. J. Bickel and K. A. Doksom, *Mathematical Statistics; Basic Ideas and Selected Topics*, Holden-Day, San Francisco, 1977.

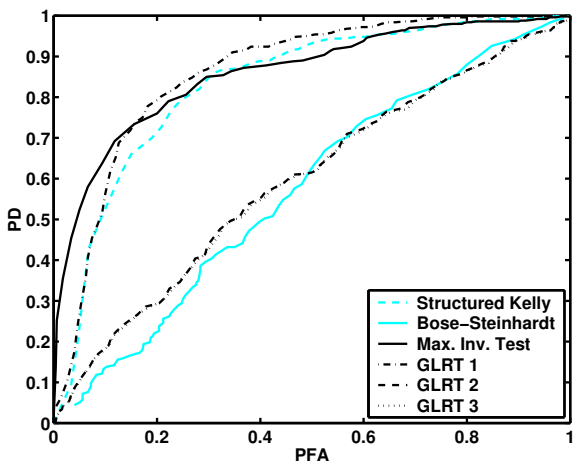

Fig. 1. ROC curves for Case I with $SNR = 23dB (SNR_A = 13dB, SNR_B = 22dB)$.

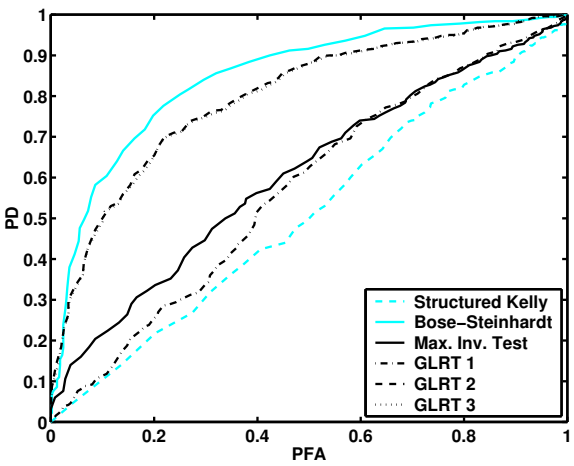

(a)

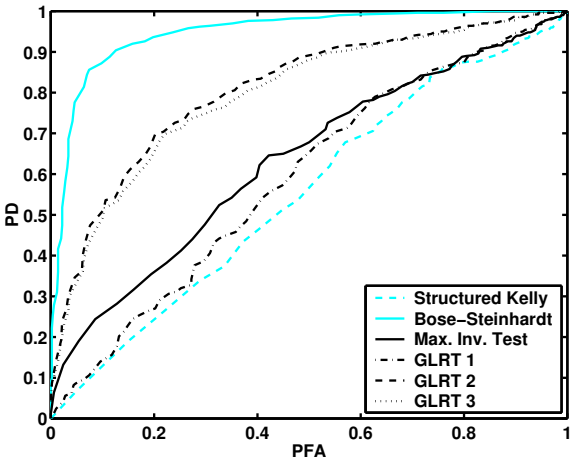

(b)

Fig. 2. ROC curves for Case II with (a) $SNR = 9dB(SNR_A = 8dB, SNR_B = 5dB)$, and (b) $SNR = 13dB(SNR_A = 8dB, SNR_B = 11dB)$.

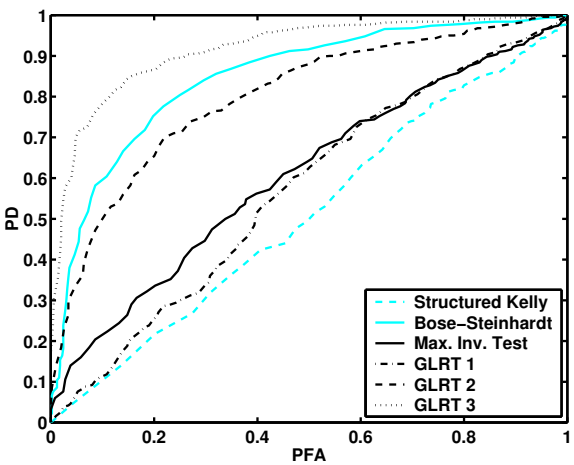

Fig. 3. ROC curves for Case III with $SNR = 9dB(SNR_A = 8dB, SNR_B = 5dB)$.

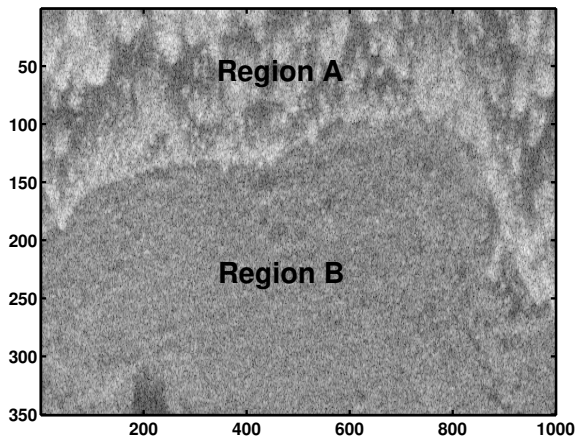

Fig. 4. SAR clutter image with a target in the boundary at column 300. This image is the rural scene near Redstone Arsenal at Huntsville, Alabama, reproduced from the data collected using the Sandia National Laboratories Twin Otter SAR sensor payload operating at X band. The data is obtained from the MSTAR SAR database at the Center for Imaging Science (www.cis.jhu.edu).

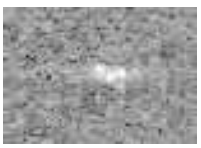

Fig. 5. SLICY canonical target image at azimuth = 163° and elevation = 39°. This is obtained from the MSTAR SAR database at the Center for Imaging Science (www.cis.jhu.edu).

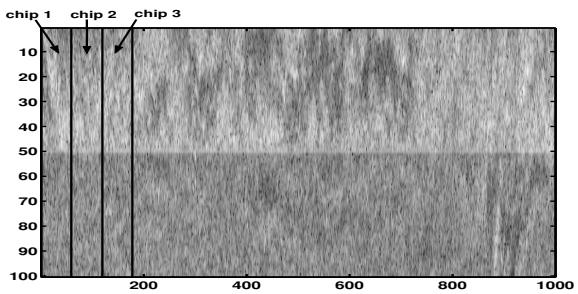

Fig. 6. Image realigned along the extracted boundary. SLICY target is located at column 300.

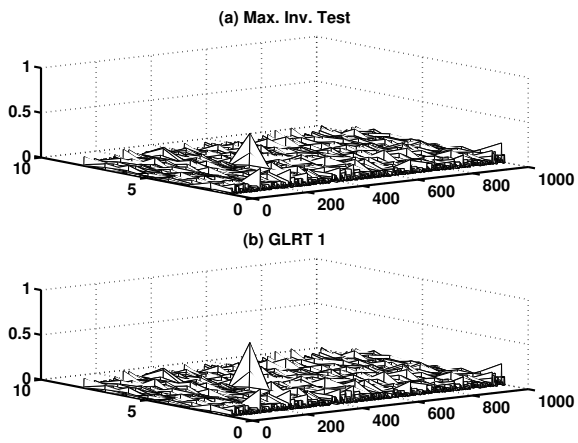

Fig. 7. Test values obtained along the boundary by (a) Maximally invariant test and (b) GLRT 1.